whether or not the test object returned to the optical trap or continued to fall.

This determination of the length of an optical trap's influence by this manner assumes that the test object falls through the water in the sample chamber at terminal velocity for the duration of its fall, so that the distance of trap influence can be computed simply by: $d = V_T t$, where d is the trap length (or distance of trap reach), V_T is the terminal velocity of the test object, and t is the time interval over which the object is allowed to fall. In order for this methodology to work, it must be established that the test object indeed falls through the water in the sample chamber at terminal velocity. This answers the question of how far below the trap point an object must be to be drawn into an optical trap in order to select and manipulate material for microscale assembly and characterization.

This methodology would make it possible for optical trapping to be incorporated into the assembly of MEMS (micro-electromechanical systems) devices. In particular, adding pieces or connectors to MEMS devices that cannot be positioned via photolithography and vapor or film deposition techniques may be added to a MEMS device via placement by optical traps. In this case, it is imperative to know how far beyond the stable trapping point in the direction of propagation of the beam an object should or must be to be trapped, and also the distance beyond the stable optical trapping point over which the propagating laser beam has no effect.

Phase-Array Approach to Optical Whispering Gallery Modulators

NASA's Jet Propulsion Laboratory, Pasadena, California

This technology leverages the well-defined orbital number of a whispering gallery modulator (WGM) to expand the range of applications for such resonators. This property rigidly connects the phase variation of the field in this mode with the azimuthal angle between the coupling locations.

A WGM with orbital momentum L has exactly L instant nodes around the circumference of the WGM resonator supporting such a mode. Therefore, in two locations separated by the arc α, the phase difference of such a field will be equal to $\phi = \alpha L$. Coupling the field out of such locations, and into a balanced interferometer, once can observe a complete constructive or distractive interference (or have any situation in between) depending on the angle α. Similarly, a mode $L + \Delta L$ will pick up the phase $\phi + \alpha \Delta L$.

In all applications of a WGM resonator as a modulator, the orbital numbers for the carrier and sidebands are different, and their differences ΔL are known (usually, but not necessarily, $\Delta L = 1$). Therefore, the choice of the angle α, and of the interferometer arms difference, allows one to control the relative phase between different modes and to perform the conversion, separation, and filtering tasks necessary.

Infrared Camera System for Visualization of IR-Absorbing Gas Leaks

This system is applicable in HVAC, methane production plants, and oil refineries.

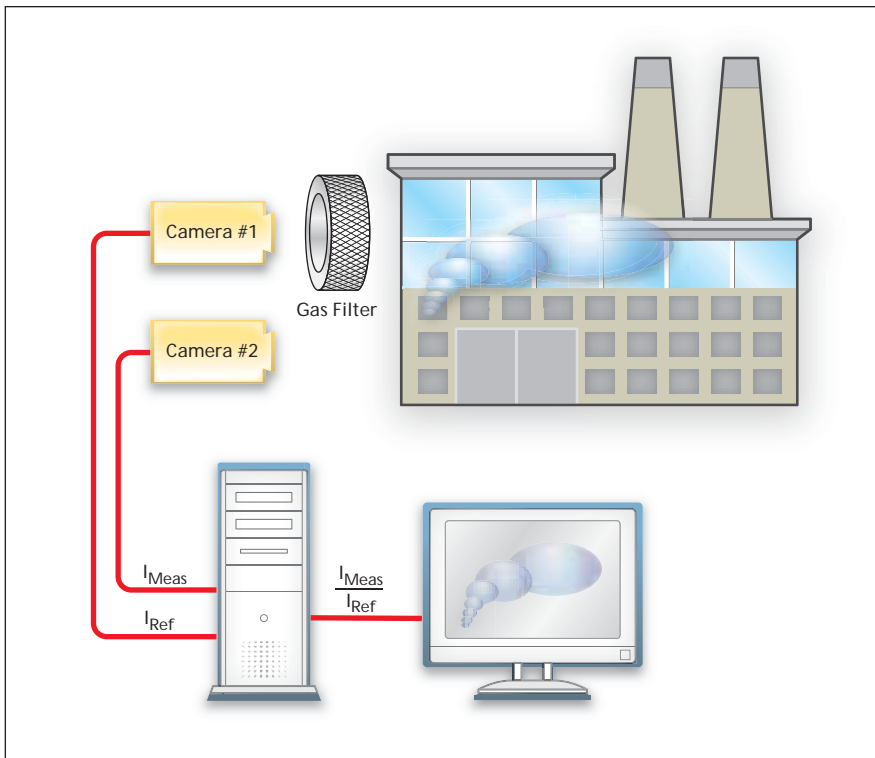*John F. Kennedy Space Center, Florida*

Leak detection and location remain a common problem in NASA and industry, where gas leaks can create hazardous conditions if not quickly detected and corrected. In order to help rectify this problem, this design equips an infrared (IR) camera with the means to make gas leaks of IR-absorbing gases more visible for leak detection and location.

By comparing the output of two IR cameras (or two pictures from the same camera under essentially identical conditions and very closely spaced in time) on a pixel-by-pixel basis, one can cancel out all but the desired variations that correspond to the IR absorption of the gas of interest. This can be simply done by absorbing the IR lines that correspond to the gas of interest from the radiation received by one of the cameras by the intervention of a filter that removes the particular wavelength of interest from the "reference" picture. This can be done most sensitively with a gas filter (filled with the gas of interest) placed in front of the IR detector array, or (less sensitively) by use of a suitable line filter in the same location.

This arrangement would then be balanced against the unfiltered "measurement" picture, which will have variations from IR absorption from the gas of interest. By suitable processing of the signals from each pixel in the two IR pictures, the user can display only the differences in the signals. Either a difference or a ratio output of the two signals is feasible. From a gas concentration viewpoint, the ratio could be processed to show the column depth of the gas leak. If a variation in the background IR light intensity is present in the field of view, then large changes in the difference signal will occur for the same gas column concentration between the background and the camera. By ratioing the outputs, the

The **Two-Camera Version of the Infrared Camera System** features two cameras with essentially the same view and time.

An alternative approach uses a simpler multiplication of the filtered signal to make the filtered signal equal to the unfiltered signal at most locations, followed by a subtraction to remove all but the wavelength-specific absorption in the unfiltered sample. This signal processing can also reveal the net difference signal representing the leaking gas absorption, and allow rapid leak location, but signal intensity would not relate solely to gas absorption, as raw signal intensity would also affect the displayed signal.

A second design choice is whether to use one camera with two images closely spaced in time, or two cameras with essentially the same view and time. The figure shows the two-camera version. This choice involves many tradeoffs that are not apparent until some detailed testing is done. In short, the tradeoffs involve the temporal changes in the field picture versus the pixel sensitivity curves and frame alignment differences with two cameras, and which system would lead to the smaller variations from the uncontrolled variables.

This work was done by Robert Youngquist and Dale Lueck of Kennedy Space Center and Christopher Immer and Robert Cox of ASRC Aerospace Corporation. Further information is contained in a TSP (see page 1). KSC-13207

same signal ratio is obtained for both high- and low-background signals, even though the low-signal areas may have greater noise content due to their smaller signal strength. Thus, one embodiment would use a ratioed output signal to better represent the gas column concentration.

Submonolayer Quantum Dot Infrared Photodetector

NASA's Jet Propulsion Laboratory, Pasadena, California

A method has been developed for inserting submonolayer (SML) quantum dots (QDs) or SML QD stacks, instead of conventional Stranski-Krastanov (S-K) QDs, into the active region of intersubband photodetectors. A typical configuration would be InAs SML QDs embedded in thin layers of GaAs, surrounded by AlGaAs barriers. Here, the GaAs and the AlGaAs have nearly the same lattice constant, while InAs has a larger lattice constant.

In QD infrared photodetector, the important quantization directions are in the plane perpendicular to the normal incidence radiation. In-plane quantization is what enables the absorption of normal incidence radiation. The height of the S-K QD controls the positions of the quantized energy levels, but is not critically important to the desired normal incidence absorption properties. The SML QD or SML QD stack configurations give more control of the structure grown, retains normal incidence absorption properties, and decreases the strain build-up to allow thicker active layers for higher quantum efficiency.

This work was done by David Z. Ting, Sumith V. Bandara, and Sarath D. Gunapala of Caltech and Yia-Chung Chang of the University of Illinois for NASA's Jet Propulsion Laboratory. Further information is contained in a TSP (see page 1). NPO-46115

Mode Tracker for Mode-Hop-Free Operation of a Laser

Lyndon B. Johnson Space Center, Houston, Texas

A mode-tracking system that includes a mode-controlling subsystem has been incorporated into an external-cavity (EC) quantum cascade laser that operates in a mid-infrared wavelength range.

The mode-tracking system makes it possible to perform mode-hop-free wavelength scans, as needed for high-resolution spectroscopy and detection of trace gases. The laser includes a gain chip, a beam-collimating lens, and a diffraction grating. The grating is mounted on a platform, the position of which can be varied to effect independent control of the EC length and the grating angle.